Korean J. Chem. Eng., 36(8), 1377-1387 (2019)
DOI: 10.1007/s11814-019-0318-7

pISSN: 0256-1115
eISSN: 1975-7220

A novel internal assistance method for enhanced fluidization of nanoparticles

Yaghoub Rahimvandi Noupoor and Maryam Tahmasebpoor†

Faculty of Chemical & Petroleum Engineering, University of Tabriz, P. O. Box 51666-16471, Tabriz, Iran
(*Received 15 November 2018 • accepted 1 June 2019*)

Abstract−Hydrophilic (polar-P) and hydrophobic (apolar-A) SiO_2 nanoparticles were used as assistant materials to improve the fluidizability of Al_2O_3 and TiO_2 nanopowders, which are hard to fluidize normally. To decrease the strong electrostatic forces, binary mixtures prepared with SiO_2(P) were fluidized in the presence of suitable alcohol vapors. Results showed that the amount of SiO_2 nanoparticles, varying from 5 to 50 wt%, mostly had a beneficial effect on the fluidization quality of the binary mixtures in both cases. TiO_2 and Al_2O_3 nanoparticles combined with 20 wt% SiO_2(A) showed almost equal performance in terms of fluidization with the mixtures containing only 5 wt% SiO_2(P). This behavior can be addressed by better material homogeneity of latter mixtures which led to a homogeneous, smooth and stable behavior with desirable bed expansion. By comparing the results obtained in this work with those available in the literature, it is proposed that physical mixing with SiO_2(P) NPs to improve the flowability of Al_2O_3 and TiO_2 hard-to-fluidize nanoparticles, may be comparatively more efficient than even some of the external methods such as acoustic field or mechanical vibration.

Keywords: Nanoparticles Fluidization, Assisted Material, Binary Mixtures, Hydrophilic SiO_2

INTRODUCTION

Fluidization is widely used for continuous powder handling in various industries, including gasification, adsorption, polymerization, and catalytic cracking [1]. Good particulate mixing and consequently favorable gas-solid contact efficiency lead fluidized powders to find these widespread applications. However, the strong interparticle forces that exist in the case of nanoparticles (NPs) and originate in their high surface-to-volume ratio, often cause undesired agglomeration. This phenomenon creates some difficulties in NPs fluidization process like severe agglomeration, channeling, reduced productivity, rat holing or even complete defluidization [2]. In this regard, handling and processing technologies of NPs to make them as highly dispersed particles as possible during the fluidization are very important factors to facilitate their industrial applications.

In general, according to Yao's definition [3], there are two types of behavior during fluidization of NPs. The first type, called agglomerate particulate fluidization (APF), is characterized by smooth and homogeneous fluidization, large values of the bed expansion ratio, bubble-free bed during fluidization and continuous increases of bed expansion with increasing superficial gas velocity. On contrary, the second type can be identified by heterogeneous fluidization, small values of the bed expansion ratio even at increased superficial gas velocity, presence of bubbles and non-uniform distribution of agglomerates. This behavior is called agglomerate bubbling fluidization (ABF) [3]. Usually, flowability of ABF-type NPs like titania and alumina can be improved by applying external or internal assisting methods. The most applicable external assisting methods include mechanical vibration [4-6], magnetic stirring [4,7,8], sound waves [9,10], pulsed flow [11,12], centrifugal fields [2,13], electric fields [14,15], and secondary gas flow from a micro-jet [16]. Although these methods enhance the fluidization behavior of NPs, external assisting methods are generally expensive and hard to scale up for industrial purposes. Therefore, it is preferred to apply the internal methods due to their low initial costs and simple procedure of scaling up. The most common internal assisting methods can be effectuated by mixing the hard-to-fluidize NPs with coarse particles such as FCC [17-19], or with secondary NPs that have better fluidization behavior such as hydrophobic silica [20,21]. These internal methods alter the intrinsic properties of fine particles by reducing the attraction forces between them. However, the method of mixing hard-to-fluidize powders with additives to enhance their fluidity may pose some practical limitations in subsequent powder processing such as film coating and hydrophobization.

As flow assistants, hydrophobic silica NPs have attracted the most attention as a reliable mixing material to improve the flowability of cohesive NPs [7,8,22-24]. For example, Valverde et al. [24] showed that mixing a Geldart C fine powder (CO_2 adsorbent) with light agglomerates of hydrophobic silica NPs serves to catalyze CO_2 adsorption in a fluidized bed by increasing fluidization homogeneity. In fact, addition of silica nanopowder helps to disperse the cohesive adsorbent aggregates, and consequently increases the effective surface area directly exposed to CO_2 and finally enables a rapid transfer of CO_2 to reactive pores [25]. In our recent papers [26,27], we improved the fluidization behavior of different CaO based sorbent particles by dry mixing with hydrophobic silica flow conditioners, which led to enhancement in CO_2 capture process. As far as untreated silica is in the form of hydrophilic, then hydrophobic silica particles are usually produced by hydrophobization of hydrophilic particles in which the hydroxyl groups are substituted by organic groups [28]. This surface modification of hydrophilic NPs using, for example, dimethyl dichlorosilane, to make them hydro-

†To whom correspondence should be addressed.
E-mail: tahmasebpoor@tabrizu.ac.ir

Table 1. Properties of the nanopowders used in this work

Commercial name	Material	Wettability	Particle diameter (nm)	Particle density (kg/m^3)	Tapped density (kg/m^3)
Aerosil® A130	SiO_2	Hydrophilic	16	2200	50
Aerosil® R972	SiO_2	Hydrophobic	16	2200	85
Aeroxide® Alu C	Al_2O_3	Hydrophilic	13	3600	60
Aeroxide® TiO_2 P25	TiO_2	Hydrophilic	21	4000	130

phobic is very complex and expensive. Therefore, it is economically preferable and incentived to use silica (P) NPs instead of silica (A) NPs to improve the flowability of hard-to-fluidize NPs. But as a drawback, the presence of hydrogen bonds between silica (P) particles makes them to be more cohesive than silica (A) NPs [29], by which the fluidization process is hindered. However, it is proved that silica (P) NPs, in the presence of 2-propanol vapor, behave almost identically to their hydrophobic counterparts in the absence of alcohol vapor. In this case, the vapor of 2-propanol alcohol binds to the surface of hydrophilic NPs by means of hydrogen bridges. After bonding, 2-propanol molecules expose their organic groups and cause to decrease the interaction between NPs, since the attraction between organic groups is weaker than that between hydroxyl groups [29].

None of the previous researches has considered the role of alcohol vapor in the fluidization mechanism of binary mixtures. In this regard, the main purpose of this research was studying the fluidization behavior of Al_2O_3(P)+SiO_2(P) and TiO_2(P)+SiO_2(P) binary mixtures in the presence of 2-propanol and methanol vapors, respectively. These two alcohols are chosen by performing fluidization experiments for individual NPs in the presence of different alcohol vapors, including methanol, 1-propanol, 2-propanol, 1-butanol and 2-butanol. In addition, the effect of weight percentage of added silica (P) NPs on flowability of the mixtures is discussed by experimental data and also Richardson-Zaki (R-Z) equation. For comparison purpose, fluidization behavior of Al_2O_3(P)+SiO_2(A) and TiO_2(P)+SiO_2(A) binary mixtures in the presence of dry nitrogen was also studied. The results are compared with the results of other researches in which the fluidization is enhanced by applying other assisting methods.

MATERIAL AND METHODS

The experiments were carried out in a fluidized bed made of a 26 mm ID and 800 mm height glass column. High purity (99.98%) nitrogen was supplied to the bed through a porous plate distributor, and alcohol vapor was added to nitrogen before it entered the bed by using a bottle filled with alcohol and kept under room temperature and ambient pressure. Five different alcohols, including methanol, 1-propanol, 2-propanol, 1-butanol and 2-butanol, which hereafter are referred to as Meth, 1Pro, 2Pro, 1But and 2But, respectively, were used in the fluidizing experiments. To avoid the emission of the NPs to the atmosphere, the gas flow leaving the bed was directed into a water bubbler and then filtered by a HEPA filter. A micro-manometer (Furness Controls, Model FM 393) was used to measure the pressure drop across the fluidized bed. This pressure drop was measured between two taps, one at the top of the column and the other located 0.02 m above the distributor.

Silica, alumina and titania NPs (all supplied by *Evonik* industry) were used in the experiments and some of their physical properties are summarized in Table 1. To avoid channeling during fluidization, large agglomerates were removed before the experiments by sieving the NPs using a 300 μm sieve placed on a shaker. As mentioned, the addition of SiO_2 NPs into the hard-to-fluidize NP beds can enhance their fluidization and reduce agglomerates elutriation rate dramatically. To reach this purpose, various mixed samples including Al_2O_3+SiO_2(P), Al_2O_3+SiO_2(A), TiO_2+SiO_2(P) and TiO_2+SiO_2(A) were prepared simply by hand dry-mixing of both powders with different weight percentages of silica NPs (5, 10, 15, 20 and 50%). By mixing, the easily fluidizable silica NP agglomerates play the role of dispersants and carriers of the Al_2O_3 and TiO_2 NPs and then the flowability of these NPs is improved. The single or binary mixed NPs were loaded to the bed up to the height of about 0.05 m.

The bed expansion ratio (H/H_0) at different superficial gas velocities and also the minimum fluidization velocity U_{mf} were studied to interpret the fluidization behavior of the particles, where H is the height of the bed at a certain superficial gas velocity and H_0 is the initial height of the bed at zero gas velocity. To yield greater consistency and repeatability of bed expansion ratios, all of the samples were fluidized initially at high velocities. After each decrease in the gas velocity, 3 minutes waiting time was taken for the bed to stabilize before the bed expansion was measured. U_{mf} was reported as the gas velocity at which an increment in the gas flow did not result in an increment in the pressure drop anymore [29]. To investigate the effect of fluidizing media on surface characteristics of individual NPs, they were taken out for FTIR analysis after being fluidized in the presence of alcohol vapors. Also, the mixing quality of binary samples was judged by scanning electron microscope (SEM) images and elemental mapping analysis obtained from energy dispersive X-ray (EDX).

RESULTS AND DISCUSSION

1. Fluidization of Individual NPs

1-1. Selection of Alcohols

Our main purpose, again, was to improve the fluidization behavior of titania and alumina NPs by adding different amounts of hydrophilic silica NPs in the presence of a suitable alcohol vapor. According to our recent work [30], different alcohols may have dissimilar effects on enhancing the flowability of cohesive hydrophilic NPs. Therefore, choosing an appropriate alcohol with the greatest influence on the fluidization quality of TiO_2, Al_2O_3 and SiO_2 NPs, would be the first step of this study. In this regard, the three men-

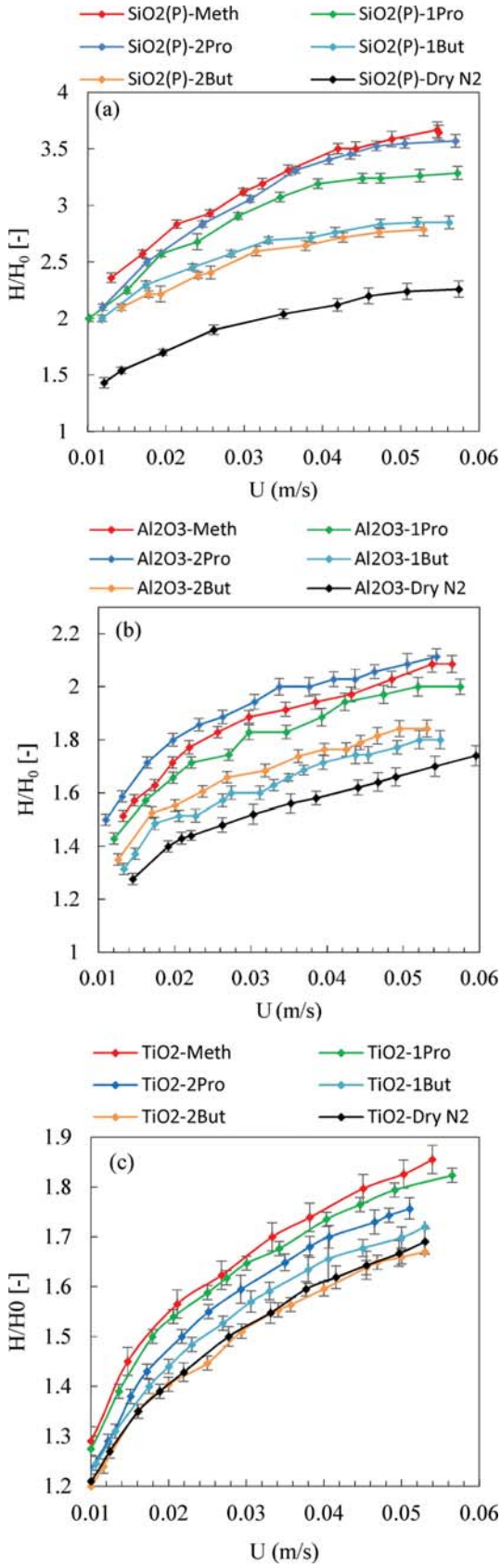

Fig. 1. Bed expansion curves for hydrophilic (a) SiO_2 (A130), (b) Al_2O_3 (AluC) and (c) TiO_2 (P25) NPs fluidized in dry nitrogen and also in the presence of different alcohols vapor.

tioned particles were fluidized individually in the presence of different alcohols, including Meth, 1-Pro, 2-Pro, 1-But and 2-But to identify the most suitable alcohol for each kind of NP. The results of the bed expansion for SiO_2(P), Al_2O_3(P) and TiO_2(P) NPs fluidized at different superficial gas velocities are shown in Figs. 1(a)-(c). These results were obtained in the absence and presence of different alcohol vapors. As can be seen, at the gas velocity of 0.05 m/s, mono component beds of SiO_2(P), Al_2O_3(P) and TiO_2(P) fluidized in dry nitrogen expanded up to about 2.24, 1.67 and 1.66-times the initial bed height, respectively. The lower expansion of Al_2O_3(P) and TiO_2(P) NPs might be attributed to their higher bulk densities and/or stronger hydrogen bridges between particles of Al_2O_3(P) and TiO_2(P) compared to SiO_2(P) [30]. Additionally, ABF behavior was observed for all three particles in the absence of alcohol vapor, which was verified by R-Z equation in the following. By adding different alcohol vapors to the fluidizing gas, the bed expansion ratio was increased in all cases, especially in the case of SiO_2(P)

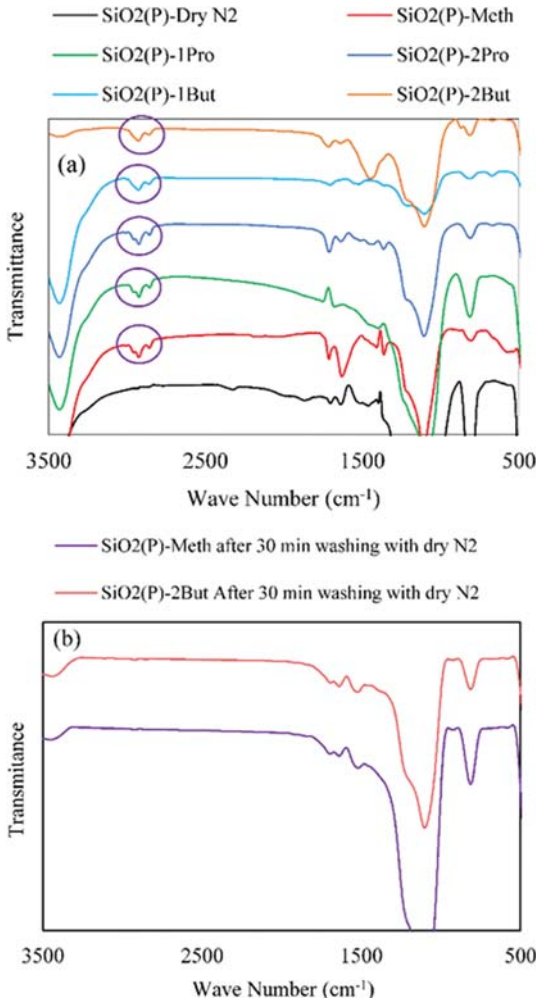

Fig. 2. FTIR transmittance spectra of the (a) SiO_2(P) NPs after being fluidized in the presence of alcohol vapor, (b) SiO_2(P) NPs after being fluidized in the presence of alcohol vapor and subsequently being washed with pure nitrogen gas. The peaks at 2,925 cm^{-1} correspond to the stretching vibration of CH_3 groups in the alcohol molecule [32].

agglomerates. In addition, there is an obvious difference between the influences of various alcohols on the fluidization behavior of NPs. The bed expansion ratio in the presence of Meth, 1-Pro, 2-Pro, 1-But, and 2-But alcohols reached to about 3.58, 3.25, 3.55, 2.85, and 2.77 for SiO_2(P) (Fig. 1(a)), reached to about 2.03, 1.97, 2.09, 1.77, and 1.84 for Al_2O_3(P) (Fig. 1(b)), and reached up to about 1.83, 1.79, 1.74, 1.70, and 1.65 for TiO_2(P) (Fig. 1(c)), respectively, in the gas velocity of 0.05 m/s.

It is believed that adding the vapor of a polar solvent like the alcohols used here to the fluidizing gas would be effective in dissipating electrostatic charges within the fluidization chamber [31]. This phenomenon happens when the polar section of the alcohol molecules weakly bind to the silanol OH groups, leaving the hydrocarbon chain to interact with other non-polar chains that consequently results in decreasing the friction of polar molecules [31]. The FTIR transmittance spectrum also confirms the adsorption of alcohol molecules by hydroxyl groups of the hydrophilic NPs. As an example, the FTIR spectra of the SiO_2(P) NPs in the presence of different alcohols are shown in Fig. 2(a). As seen, this polar particle presents peaks in the transmittance spectrum, which is consistent with the stretching vibration of the CH_3 groups in the used alcohol molecule. While, the same hydrophilic particles fluidized in dry nitrogen do not present these peaks [32]. Thus, by the adsorption of alcohol vapor, the hydrophilic SiO_2 NPs partially reform to hydrophobic, in which the process could be controlled by the type of alcohol and the gas velocity passing through the alcohol. This process is not a permanent hydrophobization and the adsorbed alcohol could be removed from the surface of NPs by washing the NPs with pure nitrogen gas. This is in agreement with the FTIR analysis results after 30 minutes washing the SiO_2(P) NPs with pure nitrogen gas (see Fig. 2(b)).

The most effective alcohols in enhancing the fluidization quality of SiO_2(P), Al_2O_3(P) and TiO_2(P) NPs can be listed as Meth, 2Pro and Meth, respectively (see Figs. 1(a)-(c)). This result might be attributed to the better bonding of the mentioned alcohols to the surface of examined NPs [30]. The results of U_{mf} also confirm all above mentioned observations, so that SiO_2(P), Al_2O_3(P) and TiO_2(P) NPs present the smallest U_{mf} in the presence of Meth, 2Pro, and Meth vapors, respectively (see Table 2). This may be caused by further reduction of the interparticle forces in the presence of these alcohols, which was studied in detail in our recent paper [30].

The fluidization behavior of NPs in the absence and presence of different alcohol vapors is also studied by the R-Z. This equation was ordinarily developed for liquid-solid systems in which the interparticle forces were neglected [33,34], but recently the modified version of this equation (which applies to NP agglomerates rather than individual NPs) has been used to investigate the degree of particulate fluidization in gas-solid systems [6,18,22,23,35,36]. The modified R-Z equation is:

$$U = U_t \varepsilon_b^n \tag{1}$$

where U is the superficial gas velocity, U_t is the terminal gas velocity, n is the R-Z exponent and ε_b is the bed voidage around the agglomerates that can be given by mass balance of the particle in the fluidized bed as:

$$\rho_a(1-\varepsilon_b)HS = \rho_{a0}(1-\varepsilon_{b0})H_0S \tag{2}$$

where ρ_a is the agglomerate density, ρ_{a0} is the agglomerate density in the condition of fixed bed, H is the bed height, H_0 is the initial bed, S is the cross sectional area of the bed and ε_{b0} is the initial bed voidage around the agglomerates. Considering the assumption that the density of the agglomerates remains almost constant before and during the fluidization ($\rho_a \approx \rho_{a0}$), Eq. (2) becomes:

$$\varepsilon_b = 1 - \frac{H_0}{H}(1-\varepsilon_{b0}) \tag{3}$$

The R-Z equation can be rewritten as the following linear equation:

$$\log U = \log U_t + n \log \varepsilon_b \tag{4}$$

where, by taking U and ε_b already known, the index n can be found.

According to Zhu et al. [36], the initial bed voidage (ε_{b0}) of APF-type SiO_2 NPs including silica R972 is within the range of 0.2 to 0.25 and then ε_{b0}=0.22 (almost the average value) was chosen for the calculations performed. As far as silica A130 in the presence of alcohol vapor presents APF behavior similar to silica R972 [29], it is reasonable to choose the same ε_{b0} value for silica A130 as well. The value of ε_{b0} for the Al_2O_3 and TiO_2 particles' bed; which exhibits higher bulk densities than that for SiO_2 particles, can be assumed 0.2 and 0.18, respectively [6,22]. A sensitivity analysis of the influence of ε_{b0} on the R-Z n exponent reveals that variations of about ±0.03 in the value of selected ε_{b0} for each NP, make negligible changes in the calculated n values. The R-Z indexes n calculated for all three

Table 2. Fluidization behavior of used nanopowders in the presence of different alcohols

	Material											
	SiO_2(P) (A130)				Al_2O_3(P) (AluC)				TiO_2(P) (P25)			
Alcohol	H/H_0[†]	U_{mf} [m/s]	n	Fluidization type	H/H_0[†]	U_{mf} [m/s]	n	Fluidization type	H/H_0[†]	U_{mf} [m/s]	n	Fluidization type
Meth	3.58	0.0075	5.503	APF	2.03	0.0213	4.297	ABF	1.83	0.0241	3.589	ABF
1Prol	3.25	0.0141	5.334	APF	1.97	0.0293	4.084	ABF	1.79	0.0254	3.556	ABF
2Pro	3.55	0.0101	5.372	APF	2.09	0.0163	4.479	ABF	1.74	0.0287	3.440	ABF
1But	2.85	0.0217	4.824	ABF	1.77	0.0384	3.566	ABF	1.70	0.0384	3.366	ABF
2But	2.77	0.0281	4.603	ABF	1.84	0.0369	3.763	ABF	1.65	0.0473	3.234	ABF
Dry N_2	2.24	0.0419	3.871	ABF	1.67	0.0401	3.300	ABF	1.66	0.0500	3.271	ABF

[†]H/H_0 obtained at U=0.05 m/s

particles during the fluidization in the presence of different alcohol vapors and also in dry nitrogen are listed in Table 2. The correlation coefficients for all the linear fitting trendlines of the experimental data are above 0.9, so all the fluidized systems obey the R-Z equation very well. It is believed that the R-Z index n of NPs can be an indicator for the characteristic of their fluidization [5,36]. The fluidization quality of APF-type NPs (such as SiO_2(A)) is ordinarily better than that of ABF-type NPs (such as Al_2O_3(P)) and consequently, these NPs present relatively higher index n compared to the ABF ones [22]. As can be seen in Table 2, the highest index n for SiO_2(P), Al_2O_3(P) and TiO_2(P) NPs is 5.503, 4.479 and 3.589, which was obtained in the presence of Meth, 2Pro and Meth vapor, respectively.

In summary, regarding this fact that the best fluidization behavior is characterized by the highest bed expansion, the maximum index n and the lowest U_{mf}, we can choose Meth, 2Pro and Meth alcohols as the most effective alcohols on improving the flowability of SiO_2(P), Al_2O_3(P) and TiO_2(P) NPs, respectively. However, as mentioned, we focused on improving the fluidization quality of binary mixtures. Therefore, the chosen alcohol was expected to have the most effect on the fluidity of hard-to-fluidize NPs (e.g., Al_2O_3(P) and TiO_2(P)). That is the reason to conduct fluidizing the binary mixtures of SiO_2(P)+Al_2O_3(P) and SiO_2(P)+TiO_2(P) in the presence of 2Pro and Meth vapors, respectively, in the following sections.

2. Fluidization of Binary Mixtures

2-1. By Adding SiO_2(P) in the Presence of Alcohol Vapor

Based on the results obtained in the previous section, monocomponent beds consisting of Al_2O_3 and TiO_2 primary NPs cannot be fluidized homogeneously because of undergoing slugging and channeling in the fluidized bed. On the other hand, SiO_2(P) NPs in the presence of alcohol vapors show better quality of fluidization with a smooth, bubble-less and homogeneous bed. Therefore, it seems that the NPs of SiO_2(P) can be used as an assistant which is able to motivate the flowability of Al_2O_3 and TiO_2 NPs. Figs. 3(a)-(b) illustrate the bed expansion curves for different content binary mixtures of Al_2O_3+SiO_2(P) and TiO_2+SiO_2(P) fluidized in the presence of 2Pro and Meth vapors, respectively. As it is obvious, by adding SiO_2(P) NPs to the beds consisting of Al_2O_3 and TiO_2 primary NPs, the bed expansion ratio increases continuously, which implies the enhancement of fluidization quality. However, the bed expansion ratio of various mixtures lies between the

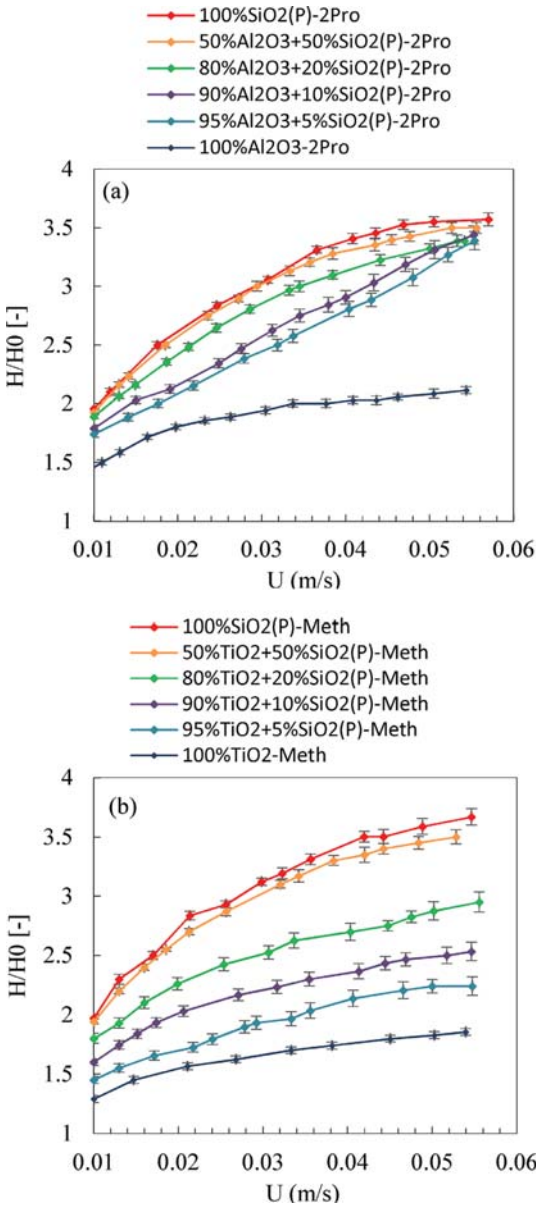

Fig. 3. Bed expansion curves for binary mixtures of (a) Al_2O_3+SiO_2(P) in the presence of 2Pro and (b) TiO_2+SiO_2(P) in the presence of Meth.

Table 3. Fluidization characteristics for binary mixtures with different weight percentage of SiO_2(P) NPs

Binary mixture	Al_2O_3+SiO_2(P)			TiO_2+SiO_2(P)		
Alcohol	2Pro			Meth		
SiO_2(P) wt%	U_{mf} [m/s]	n	Fluidization type	U_{mf} [m/s]	n	Fluidization type
0†	0.0401	3.300	ABF	0.0500	3.271	ABF
0	0.0163	4.479	ABF	0.0241	3.589	ABF
5	0.0158	4.934	ABF	0.0210	4.075	ABF
10	0.0146	5.093	APF	0.0196	4.611	ABF
20	0.0134	5.164	APF	0.0179	5.234	APF
50	0.0125	5.268	APF	0.0163	5.401	APF
100	0.0101	5.372	APF	0.0075	5.503	APF

†Fluidized TiO_2 or Al_2O_3 NPs with dry N_2

bed expansion ratio of individual constituents. As the fraction of SiO_2(P) NPs increases, the expansion behavior of fluidized mixture resembles more closely that of individual SiO_2(P) nanopowder. As shown in Fig. 3(a), in the presence of 2Pro and at the gas velocity of 0.05 m/s, the bed expansion ratio for the binary mixtures of Al_2O_3+SiO_2(P) with silica weight percentages of 5, 10, 20 and 50% reaches 3.16, 3.28, 3.32 and 3.46, respectively. Also, at the same gas velocity and in the presence of Meth, the bed expansion ratio for the binary mixtures of TiO_2+SiO_2(P) with silica weight percentages of 5, 10, 20 and 50% reaches 2.24, 2.48, 2.86 and 3.47, respectively (see Fig. 3(b)). The obtained U_{mf} values for the blended mixtures (listed in Table 3) also reveal that by increasing the fraction of SiO_2(P) in the mixtures, the value of U_{mf} decreases, which indicates the enhancement of fluidization behavior.

The superior fluidization performance of Al_2O_3+SiO_2(P) binary mixtures compared to the binary mixtures of TiO_2+SiO_2(P), under the same condition, might be attributed to the different nature of NPs and intrinsic higher density of TiO_2 NPs compared to Al_2O_3 NPs. This is consistent with Yao's remarks [3], which shows that NPs with higher densities have lower bed expansions and consequently show ABF behavior during fluidization. Note that even adding only 5% of SiO_2(P) NPs to the Al_2O_3 and TiO_2 primary particles leads to a notable increase in their bed expansion ratio. According to visual observations, by adding SiO_2(P) to the mixtures and fluidizing them in the presence of alcohol vapor, the cohesion of NPs to the bed wall disappears. This leads to a homogeneous, smooth and stable behavior with a desirable bed expansion in fluidized conditions even at low superficial gas velocities. Fig. 4 shows the fluidization behavior of TiO_2 NPs, which are the hardest to fluidize, with different amounts of SiO_2(P) in the presence of Meth vapor and at the medium gas velocity of 0.03 m/s. As can be seen, the channeling of bed during fluidization process is hindered for all cases by using hydrophilic SiO_2 as an aid additive.

As further study, the fluidization behavior of all binary mixtures, prepared by adding SiO_2(P) NPs in the presence of alcohol vapor, was analyzed by the R-Z model. The R-Z indexes n of the binary mixtures are listed in Table 3. According to the table, the value of n increases continuously by increasing the fraction of SiO_2(P) NPs in the mixtures, under the same range of superficial gas velocity. As already discussed, the increment of index n implies the improvement of fluidization behavior; i.e., the larger the index n, the smoother and more homogeneous the fluidization. Therefore, it can be concluded that Al_2O_3 and TiO_2 NPs, which present ABF behavior when used as single powders, generally show APF behavior by adding SiO_2(P) NPs except for the samples of 95%Al_2O_3+5%SiO_2(P), 95%TiO_2+5%SiO_2(P) and 90%TiO_2+10%SiO_2(P) which show ABF behaviors (see Table 3).

2-2. By Adding SiO_2(A) in the Presence of Dry Nitrogen

SiO_2(A) is used as a common auxiliary material to enhance the fluidization of hard-to-fluidize NPs. Therefore, we decided to flu-

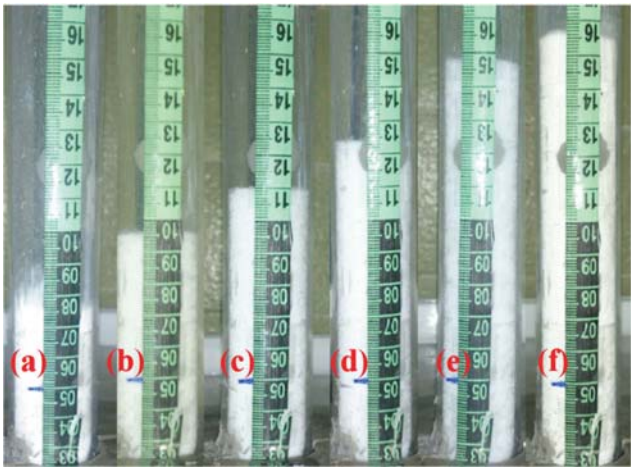

Fig. 4. Fluidization behavior of individual TiO_2 (a), TiO_2+SiO_2(P) binary mixtures with silica weight percentage of 5% (b), 10% (c), 20% (d), 50% (e) and individual SiO_2(P) (f); in the presence of Meth vapor and at the gas velocity of 0.03 m/s.

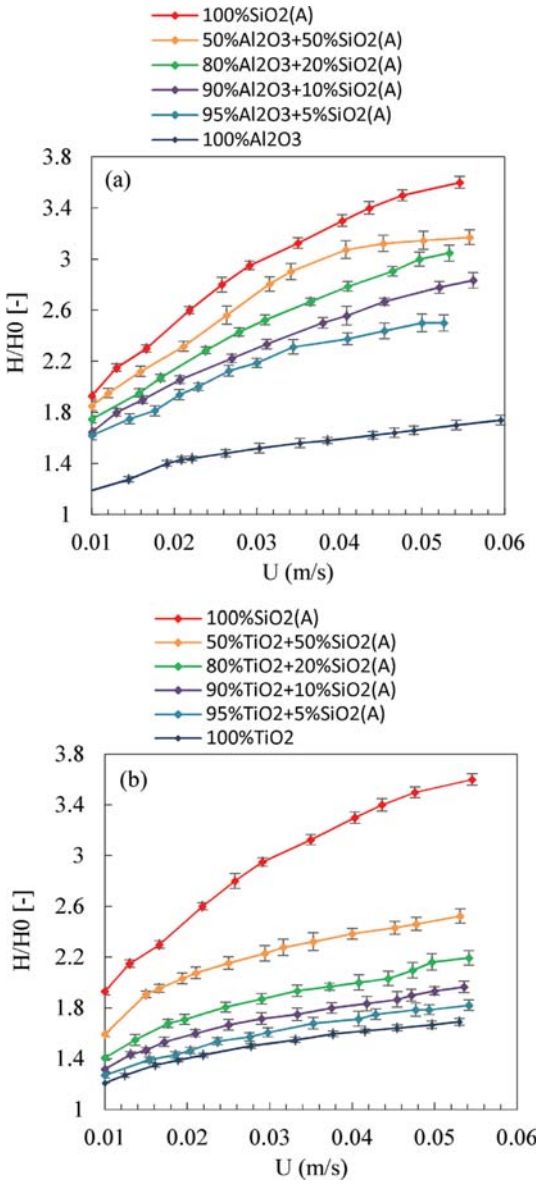

Fig. 5. Bed expansion curves for binary mixtures of (a) Al_2O_3+SiO_2(A) and (b) TiO_2+SiO_2(P) in the presence of dry nitrogen gas.

Table 4. Fluidization characteristics for binary mixtures with different weight percentage of SiO_2(A) NPs

Binary mixture	Al_2O_3+SiO_2(A)			TiO_2+SiO_2(A)		
SiO_2(A) wt%	U_{mf} [m/s]	n	Fluidization type	U_{mf} [m/s]	n	Fluidization type
0	0.0401	3.300	ABF	0.0500	3.271	ABF
5	0.0362	4.673	ABF	0.0429	3.457	ABF
10	0.0316	4.861	ABF	0.0353	3.704	ABF
20	0.0238	4.932	ABF	0.0294	3.995	ABF
50	0.0184	5.139	APF	0.0230	4.597	ABF
100	0.006	5.346	APF	0.006	5.346	APF

idize different amount binary mixtures of Al_2O_3+SiO_2(A) and TiO_2+SiO_2(A) in dry nitrogen to observe their typical ABF or APF behavior. Figs. 5(a)-(b) show the bed expansion curves for the mentioned mixtures with different weight percentages of SiO_2(A). Similar to the previous section, mixtures with the highest amount of SiO_2(A), Al_2O_3 or TiO_2 behave like the powders alone and mixtures with an intermediate composition have an intermediate behavior in terms of bed expansion. Also, the fluidization quality of the mixtures is generally improved by increasing the amount of SiO_2(A) NPs. This is mainly because of the better fluidization quality of SiO_2(A) NPs compared to the other constituent of the mixture, at the same fluidization conditions. From Fig. 5(a), at the gas velocity of 0.05 m/s, the bed expansion ratio for the Al_2O_3+SiO_2(A) binary mixtures with silica weight percentages of 5, 10, 20 and 50% SiO_2(A) is 2.50, 2.74, 3.00 and 3.14, respectively. Also, at the same conditions, the bed expansion ratio for the binary mixtures of TiO_2+SiO_2(A) reaches 1.80, 1.92, 2.16 and 2.48, respectively (see Fig. 5(b)). These bed expansion values are considerably lower than those obtained by adding SiO_2(P) NPs, which will be discussed more in the following section. Also, a modest fluidization improvement by increasing the percentage of SiO_2(A) is clear by U_{mf} results, i.e., the more amount of SiO_2(A) in the mixtures, the lower U_{mf} (see Table 4). Moreover, the comparison between the curves of Figs. 5(a) and 5(b) reveals that the Al_2O_3 NPs are affected more than TiO_2 NPs by the addition of SiO_2(A). As discussed in the previous section, this superior behavior might be attributed to the difference in the nature of NPs and the difference in the density of Al_2O_3 and TiO_2 NPs; (i.e., the Al_2O_3 NPs have lower density compared toTiO_2 NPs (see Table 1)). NPs with higher densities have lower bed expansions [3] and consequently, more silica additive is needed to increase their bed expansion ratio.

Based on visual observations, plug formation and/or channeling behavior are observed at low gas velocities (lower than 0.02 m/s) during the fluidization process of Al_2O_3+SiO_2(A) and TiO_2+SiO_2(A) mixtures. In some cases, half of the bed rises integrated like a piston and by gradually increasing the gas velocity the plug breaks and the mixture collapses to fluidize normally. At medium gas velocities (0.02 to 0.03 m/s) usually the top of the bed begins to fluidize, whereas the bottom of the bed is kept as a fixed bed, which may be due to the formation of larger agglomerates in the bottom part of the bed. An increase in SiO_2(A) content results in higher bed expansion at the similar condition and the same gas velocity. Fig. 6 shows the bed expansion trend by increasing the SiO_2(A) content in TiO_2+SiO_2(A) mixtures at the constant gas velocity of 0.03 m/s.

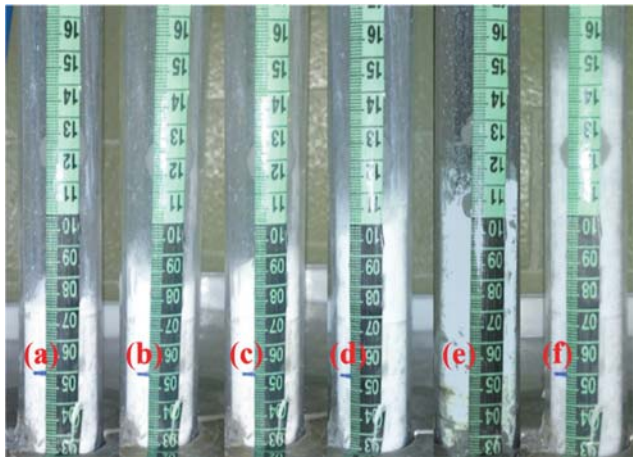

Fig. 6. Fluidization behavior of individual TiO_2 (a), TiO_2+SiO_2(A) binary mixtures with silica weight percentage of 5% (b), 10% (c), 20% (d), 50% (e) and individual SiO_2(A) (f); in the presence of dry nitrogen gas and at the gas velocity of 0.03 m/s.

Using the R-Z equation, the particulate fluidization degree of all binary mixtures, prepared by adding SiO_2(A) NPs, is investigated. The calculated index n for all prepared samples are listed in Table 4. As is obvious, increasing the fraction of SiO_2(A) in the mixtures leads to the increase of the R-Z exponent n as well. Although, the increment of n by increasing the amount of SiO_2(A) assistant NPs shows the improvement of fluidization quality of the mixtures, but they rarely show APF behavior based on the visual observations. All of the SiO_2(A)-assisted samples except 50%Al_2O_3+50%SiO_2(A), show ABF behavior during the fluidization procedure.

3. Comparison of the Results

Here, we show the bed expansion comparison of SiO_2(P) and SiO_2(A) contain mixtures during fluidization by dry nitrogen or nitrogen containing alcohol vapor. Figs. 7(a)-(b) present the bed expansion curves for different content binary mixtures of TiO_2+SiO_2 and Al_2O_3+SiO_2, respectively. As can be seen, TiO_2 NPs mixed with 20 and 50 wt% SiO_2(A) show almost equal fluidization performance with those mixed with only 5 and 10 wt% SiO_2(P) in the presence of Meth vapor, respectively (Fig. 7(a)). Also, the bed expansion ratios for the Al_2O_3+SiO_2(A) binary mixtures with silica weight percentage of 20 and 50% are approximately equal to those of Al_2O_3+SiO_2(P) binary mixtures with silica weight percentages of only 5 and 15% in the presence of 2Pro vapor, respectively (Fig. 7(b)). The better fluidization behavior of blended samples with SiO_2(P) rather

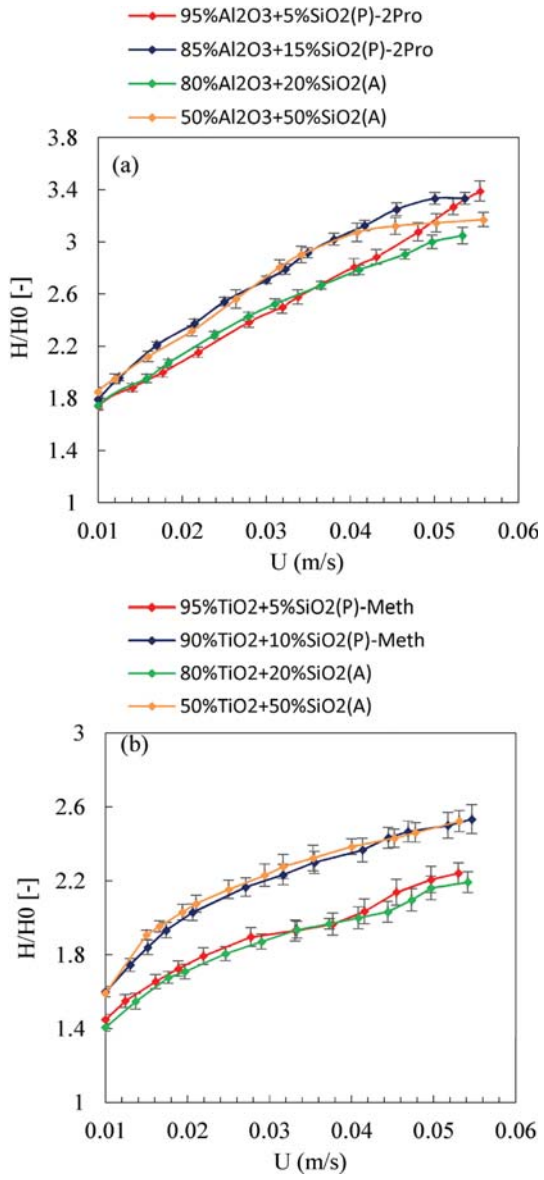

Fig. 7. Comparing the bed expansions during fluidization of (a) Al_2O_3 and (b) TiO_2 mixed with SiO_2(P) and SiO_2(A).

than SiO_2(A) is more clear by comparing the corresponding U_{mf} results, i.e., mixtures containing SiO_2(P) have considerably lower U_{mf} values compared to those of SiO_2(A) assisted mixtures according to Tables 3 and 4. Furthermore, the R-Z calculations also confirm the higher fluidization performance of Al_2O_3+SiO_2(P) and TiO_2+SiO_2(P) binary mixtures in the presence of nitrogen containing alcohol vapors rather than that of Al_2O_3+SiO_2(A) and TiO_2+SiO_2(A) ones in the presence of dry nitrogen. It means that the index n for mixtures containing SiO_2(P) is relatively higher than that for the mixtures containing SiO_2(A) with the same composition (see Tables 3 and 4). These results clarify the more effectiveness of SiO_2(P) assistant NPs in enhancing the fluidization behavior of hard-to-fluidize particles rather than SiO_2(A). In this regard, the index n for pure SiO_2(A) NPs fluidized in dry nitrogen is approximately 5.346, while it is 5.503 and 5.372 for pure SiO_2(P) NPs fluidized in nitrogen containing Meth and 2Pro vapors, respectively (see Table 3 and 4).

To justify the results, SEM images and elemental mapping analyses of a random agglomerate taken from four different samples, 80%Al_2O_3+20%SiO_2(P), 80%Al_2O_3+20%SiO_2(A), 80%TiO_2+20%SiO_2(P) and 80%TiO_2+20%SiO_2(A), were studied (see Figs. 8(a)-(d)). The elemental mapping images show the distribution scale of Al, Ti and Si elements, which are indicative for the distribution scale of Al_2O_3, TiO_2 and SiO_2, respectively. Based on these images, it is clear that Al_2O_3 and TiO_2 agglomerates are well mixed with silica NPs despite the break-up and reforming cycle of agglomerates in fluidized bed, which means easily fluidizable SiO_2 NPs play the role of carriers for hard-to-fluidize Al_2O_3 and TiO_2 agglomerates during fluidization. Considering the SEM images along with the distribution shape of Si element, it is clear that SiO_2(P) additive NPs tend to adhere to the Al_2O_3 and TiO_2 agglomerates (see Figs. 8(a) and (c)); however, SiO_2(A) additive NPs are scattered inside the bulk of material (see Figs. 8(b) and (d)). Therefore, it may be concluded that the established force between hard-to-fluidize agglomerates and SiO_2(P) is stronger than that of SiO_2(A) NPs. Moreover, in the presence of SiO_2(A) NPs, the mixed particles have a poor coverage of the materials over each other (Figs. 8(b) and 8(d)). This result is in agreement with the result obtained by van der Vegte and Hadziioannou [37]. They declare that the mean adhesion force between two hydroxyl groups is 0.9 nN, and it is only 0.3 nN between an alkyl group and a hydroxyl group. This means that SiO_2(P) NPs, with hydroxyl groups, are able to bind on the surface of hydrophilic alumina and titania agglomerates better than SiO_2(A) NPs with alkyl groups. Although the SiO_2(P) NPs partially reform to hydrophobic in the presence of alcohols, the generated steric repulsion may be still relatively lower than that between SiO_2(A) NPs.

The visual observations during experiments were also used as a good insight into the fluidization behavior of the mixtures containing SiO_2(P) or SiO_2(A) NPs. By comparing Figs. 4 and 6, mixtures containing SiO_2(A) show poor streaming quality, performance fluctuations and also lower bed expansions compared to SiO_2(P) containing mixtures under the same conditions. These figures illustrate that SiO_2(P) assisted mixtures generally have smoother fluidization with a specific bed surface, while SiO_2(A) assisted mixtures have an irregular bed surface caused by rapid bed fluctuations. Other observations show that SiO_2(A) assisted mixtures usually show channeling and plugging behaviors at low gas velocities (lower than 0.02 m/s). However, SiO_2(P) assisted mixtures fluidize smoothly without any channeling behavior even at low gas velocities. The fluidization behavior (i.e., APF or ABF) of the blended samples is determined mostly by visual observations [3]. As an example, the sample 80%TiO_2+20%SiO_2(P) in the presence of methanol vapor is smoothly fluidized with high bed expansion ratios (see Fig. 3(b)) and no bubbles spotted, which is indicative of APF behavior. In reverse, the sample 80%TiO_2+20%SiO_2(A) is fluidized heterogeneously with lower bed expansion ratios (see Fig. 5(b)) and large bubbles, which is known as ABF behavior. Furthermore, the R-Z calculations confirm the observational fluidization types of blended samples (i.e., the index n of APF NPs is relatively higher compared with ABF NPs [22]). Although elutriation is observed for both types

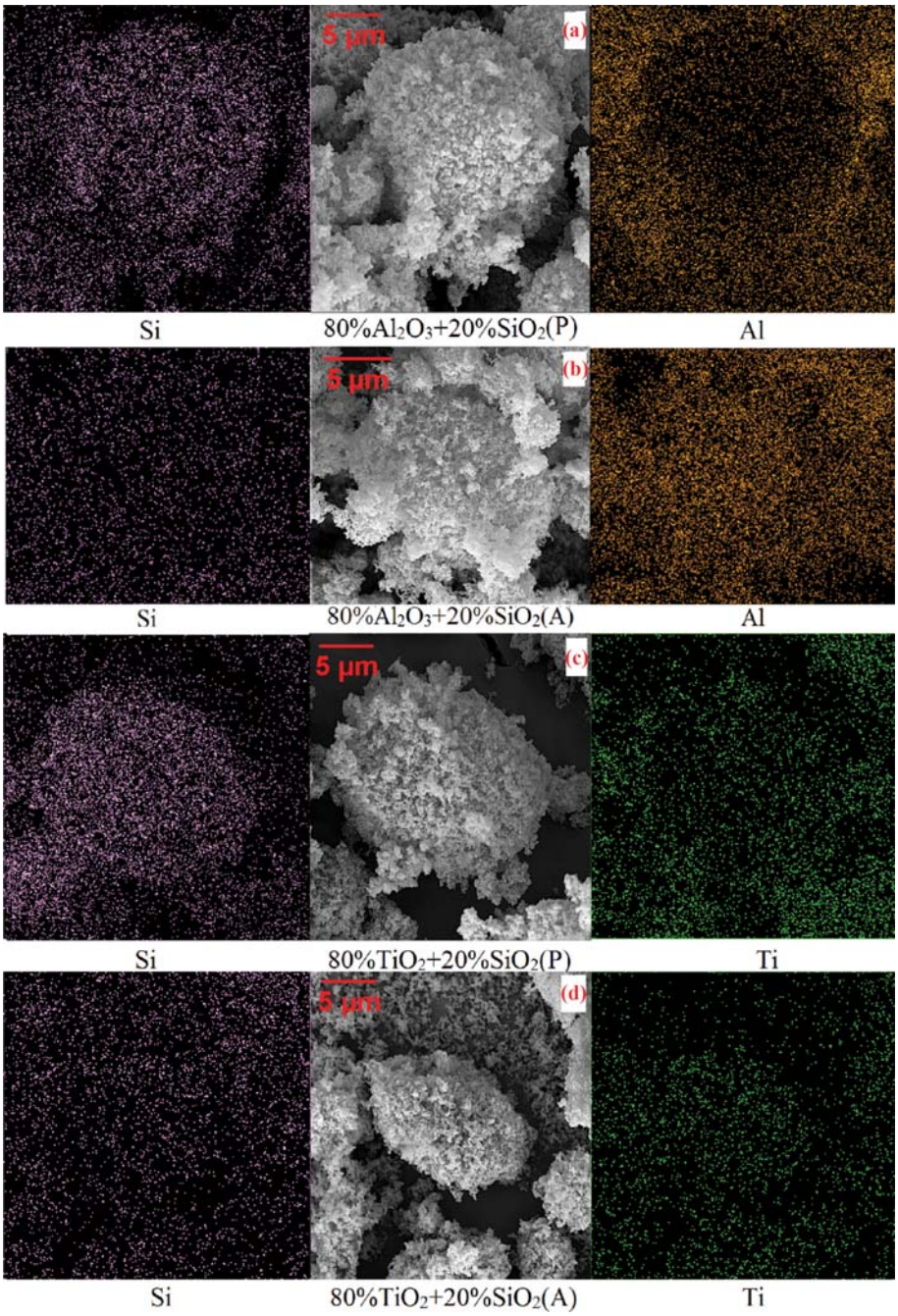

Fig. 8. SEM and elemental mapping images of the samples (a) 80%Al_2O_3+20%SiO_2(P), (b) 80%Al_2O_3+20%SiO_2(A), (c) 80%TiO_2+20%SiO_2(P) and (d) 80%TiO_2+20%SiO_2(A).

of the blended samples at high gas velocities (higher than approximately 0.04 m/s), it seems more significant in the case of SiO_2(A) assisted mixtures. At lower gas velocities, elutriation is rarely observed for blended samples with SiO_2(P) aid additive while SiO_2(A) assisted mixtures are elutriated which is somehow clear in Fig. 6. Generally, increasing the fraction of SiO_2(P) in the mixtures reduces the rate of their elutriation, but we did not spot any changes in the elutriation rate of the mixtures prepared by addition of SiO_2(A) NPs.

Finally, the results obtained in this work were compared with those reported in the literature for other assistance methods. Tables 5 and 6 show the effect of applying different assistance methods on H/H_0 in the beds of Al_2O_3 and TiO_2 NPs, respectively. Due to the different ranges of gas velocity in the experiments, we decided to compare the bed expansions in a specific gas velocity. However, this comparison may not be fair because the authors have not used the same type of alumina and titania NPs, but it definitely gives an approximate insight to compare the results. It can be seen from these tables that most of the researchers apply an external method or a combination of external and internal methods as an assistant to enhance the fluidization of Al_2O_3 and TiO_2 NPs. This implies

Table 5. Comparing the bed expansion results of this work with those reported in the literature for Al_2O_3 NPs

Reference	Method	U [m·s^{-1}]	Additive	H/H$_0$
[16]	Micro-jet	0.030	-	11.39
This work		0.030	50% Hydrophilic SiO_2+2Pro	3.02
[7]	Magnetic field	0.013	50% Hydrophobic SiO_2	4.50
This work		0.013	50% Hydrophilic SiO_2+2Pro	2.15
[8]	Magnetic field	0.014	67% Hydrophobic SiO_2	3.39
This work		0.014	50% Hydrophilic SiO_2+2Pro	2.23
[7]	Magnetic field	0.0194	-	2.99
This work		0.0194	50% Hydrophilic SiO_2+2Pro	2.55
[38]	Acoustic field	0.01	50% Fe_2O_3	1.72
[38]	Acoustic field	0.01	-	1.53
[10]	Acoustic field	0.01	-	1.18
This work		0.01	50% Hydrophilic SiO_2+2Pro	1.74

Table 6. Comparing the bed expansion results of this work with those reported in the literature for TiO_2 NPs

Source	Method	U [m·s^{-1}]	Additive	H/H$_0$
[16]	Micro-jet	0.03	-	6.46
This work		0.03	50% Hydrophilic SiO_2+Meth	3.03
[8]	Magnetic field	0.0141	67% Hydrophobic SiO_2	4.02
This work		0.0141	50% Hydrophilic SiO_2+Meth	2.26
[22]	Mechanical vibration	0.03	50% Hydrophobic SiO_2	1.90
[23]	Mechanical vibration	0.03	50% Fe_2O_3	1.64
[6]	Mechanical vibration	0.03	-	1.18
[10]	Acoustic field	0.03	-	1.34
[39]	-	0.03	30% Hydrophobic SiO_2, 45% FCC	1.28
[18]	-	0.03	40% FCC	1.06
[17]	-	0.03	Unknown amount of FCC	1.16
This work			5% Hydrophilic SiO_2+Meth	1.95

that the internal methods used in the literature would have not been effective enough to improve the fluidization of hard-to-fluidize NPs. While the internal assistance method proposed in this work (i.e., adding SiO_2(P) in the presence of alcohol vapor), seems to be more effective than even external methods like applying acoustic field or mechanical vibration. It also gives better results compared to the case when the particles are mixed with FCC, Fe_2O_3 or SiO_2(A), at the same gas velocity. For instance, at the gas velocity of 0.03 m/s, the bed expansion ratio of TiO_2 NPs mixed with 5 wt% SiO_2(P) fluidized in the presence of Meth alcohol reaches 1.95, and it reaches 1.90 by adding 50% SiO_2(A) NPs and applying mechanical vibration simultaneously [22]. However, in the case of Al_2O_3 and TiO_2 NPs' fluidization has considerably higher performance compared to the other assistance methods including the proposed method in this paper.

CONCLUSION

The fluidization behavior of three different hydrophilic nano-sized powders, SiO_2, Al_2O_3 and TiO_2, as fluidized individually in the presence of different alcohol vapors (Meth, 1Pro, 2Pro, 1But and 2But), was first characterized. Although ABF-behavior was observed for all three single particles in the absence of alcohol vapor, in particular SiO_2 exhibited a better fluidization quality than the others. Among all used alcohols, Meth, 2Pro and Meth were the most effective ones on fluidization improvement of SiO_2, Al_2O_3 and TiO_2 NPs, respectively.

For the first time, the fluidization characteristics of the binary mixtures of Al_2O_3+SiO_2(P) and TiO_2+SiO_2(P) were also investigated when the fluidizing gas was vaporized with alcohol. Generally, the Richardson-Zaki index n of the binary mixtures increased with increasing the mass fraction of SiO_2 varying from 5 to 50 wt%. Adding only 5 wt% of SiO_2(P) to the Al_2O_3 and TiO_2 NPs, resulted in easier and more uniform fluidization. Linear regression of R-Z equation for the mixtures fluidized in the presence of alcohol vapors showed that ABF-behavior of Al_2O_3 and TiO_2 NPs turned to APF-behavior by adding only 10 and 20 wt% SiO_2(P), respectively. It was concluded that the internal assisting method proposed in this work (i.e., adding SiO_2(P) in the presence of alcohol vapor) may be more influential on enhancing the fluidization quality of hard-to-fluidize NPs rather than adding FCC coarse particles or Fe_2O_3 and SiO_2(A) NPs, and also some external methods like applying acoustic field or mechanical vibration. However, micro-jet and magnetic field assisted fluidization have consider-

ably higher performance compared to the other assisting methods including the proposed method in this paper.

CONFLICT OF INTEREST

The authors declare that they have no conflict of interest.

REFERENCES

1. M. Aghabararnejad, N. Mostoufi, R. Sotudeh-Gharebagh and R. Zarghami, *Ind. Eng. Chem. Res.*, **50**, 4245 (2011).
2. S. Matsuda, H. Hatano, T. Muramoto and A. Tsutsumi, *AIChE J.*, **50**, 2763 (2004).
3. W. Yao, G. Guangsheng, W. Fei and W. Jun, *Powder Technol.*, **124**, 152 (2002).
4. Q. Yu, R. N. Dave, C. Zhu, J. A. Quevedo and R. Pfeffer, *AIChE J.*, **51**, 1971 (2005).
5. C. H. Nam, R. Pfeffer, R. N. Dave and S. Sundaresan, *AIChE J.*, **50**, 1776 (2004).
6. J. Yang, T. Zhou and L. Song, *Adv. Powder Technol.*, **20**, 158 (2009).
7. J. V. Scicolone, D. Lepek, L. Louie and R. N. Davé, *J. Nanopart. Res.*, **15**, 1434 (2013).
8. P. Zeng, T. Zhou and J. Yang, C*hem. Eng. Processing: Process Intensification*, **47**, 101 (2008).
9. C. Zhu, G. Liu, Q. Yu, R. Pfeffer, R. N. Dave and C. H. Nam, *Powder Technol.*, **141**, 119 (2004).
10. S. Kaliyaperumal, S. Barghi, J. Zhu, L. Briens and S. Rohani, *Powder Technol.*, **210**, 143 (2011).
11. S. S. Ali and M. Asif, *Powder Technol.*, **225**, 86 (2012).
12. H. Khosravi Bizhaem and H. Basirat Tabrizi, *Powder Technol.*, **237**, 14 (2013).
13. H. Nakamura and S. Watano, *Powder Technol.*, **183**, 324 (2008).
14. M. Kashyap, D. Gidaspow and M. Driscoll, *Powder Technol.*, **183**, 441 (2008).
15. J. M. Valverde, M. A. Quintanilla, M. J. Espin and A. Castellanos, *Phys. Rev. E Stat. Nonlin. Soft. Matter. Phys.*, **77**, 031301 (2008).
16. J. A. Quevedo, A. Omosebi and R. Pfeffer, *AIChE J.*, **56**, 1456 (2010).
17. J. Wang, B. Xu, T. Zhou and X. Liang, *Chem. Eng. Technol.*, **39**, 1490 (2016).
18. L. Song, T. Zhou and J. Yang, *Adv. Powder Technol.*, **20**, 366 (2009).
19. H. Duan, X. Liang, T. Zhou, J. Wang and W. Tang, *Powder Technol.*, **267**, 315 (2014).
20. Y. Chen, J. Yang, R. N. Dave and R. Pfeffer, *AIChE J.*, **54**, 104 (2008).
21. J. Yang, A. Sliva, A. Banerjee, R. N. Dave and R. Pfeffer, *Powder Technol.*, **158**, 21 (2005).
22. X. Liang, H. Duan, T. Zhou and J. Kong, *Adv. Powder Technol.*, **25**, 236 (2014).
23. X. Liang, Y. Zhou, L. Zou, J. Kong, J. Wang and T. Zhou, *Powder Technol.*, **304**, 101 (2016).
24. J. M. Valverde, F. Pontiga, C. Soria-Hoyo, M. A. Quintanilla, H. Moreno, F. J. Duran and M. J. Espin, *Phys. Chem. Chem. Phys.*, **13**, 14906 (2011).
25. M. A. S. Quintanilla and J. M. Valverde, *Particuology*, **11**, 448 (2013).
26. B. Azimi, M. Tahmasebpoor, P. E. Sanchez-Jimenez, A. Perejon and J. M. Valverde, *Chem. Eng. J.*, **358**, 679 (2018).
27. O. Amjadi, M. Tahmasebpoor and H. Aghdasinia, *Chem. Eng. Technol.*, **42**, 287 (2019).
28. F. Pontiga, J. Valverde, H. Moreno and F. Duran-Olivencia, *Chem. Eng. J.*, **222**, 546 (2013).
29. M. Tahmasebpoor, L. de Martín, M. Talebi, N. Mostoufi and J. R. van Ommen, *PCCP*, **15**, 5788 (2013).
30. M. Tahmasebpoor, R. Ghasemi Seif Abadi, Y. Rahimvandi Noupoor and P. Badamchizadeh, *Ind. Eng. Chem. Res.*, **55**, 12939 (2016).
31. R. Pfeffer and J. A. Quevedo, US Patent, 7,905,433 (2011).
32. P. Larkin, Infrared and Raman spectroscopy; principles and spectral interpretation, Elsevier (2011).
33. J. Chaouki, C. Chavarie, D. Klvana and G. Pajonk, *Powder Technol.*, **43**, 117 (1985).
34. J. M. Valverde and A. Castellanos, *Powder Technol.*, **181**, 347 (2008).
35. L. de Martín and J. R. van Ommen, *J. Nanopart. Res.*, **15**, 1 (2013).
36. C. Zhu, Q. Yu, R. N. Dave and R. Pfeffer, *AIChE J.*, **51**, 426 (2005).
37. E. W. van der Vegte and G. Hadziioannou, *Langmuir*, **13**, 4357 (1997).
38. P. Ammendola, R. Chirone and F. Raganati, *Adv. Powder Technol.*, **22**, 174 (2011).
39. H. Duan, J. Wang and T. Zhou, *Procedia Eng.*, **102**, 815 (2015).